Atmospheric Environment 153 (2017) 32–40

Contents lists available at ScienceDirect

Atmospheric Environment

journal homepage: www.elsevier.com/locate/atmosenv

# Atmospheric nitrogen deposition to China: A model analysis on nitrogen budget and critical load exceedance

Yuanhong Zhao [a], Lin Zhang [a,*], Youfan Chen [a], Xuejun Liu [b], Wen Xu [c], Yuepeng Pan [d], Lei Duan [e]

[a] Laboratory for Climate and Ocean-Atmosphere Sciences, Department of Atmospheric and Oceanic Sciences, School of Physics, Peking University, Beijing 100871, China
[b] College of Resources and Environmental Sciences, China Agricultural University, Beijing 100193, China
[c] State Key Laboratory of Urban and Regional Ecology, Research Center for Eco-Environmental Sciences, Chinese Academy of Sciences, Beijing 100085, China
[d] State Key Laboratory of Atmospheric Boundary Layer Physics and Atmospheric Chemistry (LAPC), Institute of Atmospheric Physics, Chinese Academy of Sciences, Beijing 100029, China
[e] State Key Joint Laboratory of Environmental Simulation and Pollution Control, School of Environment, Tsinghua University, Beijing, 100084, China

## HIGHLIGHTS

- Sources and processes controlling nitrogen deposition over China are quantified.
- Reduced nitrogen ($NH_3$) and dry deposition process are significant contributors.
- 15% of the China's land experiences critical load exceedances for eutrophication.

## ARTICLE INFO

*Article history:*
Received 26 September 2016
Received in revised form
5 January 2017
Accepted 7 January 2017
Available online 8 January 2017

*Keywords:*
Nitrogen deposition
Nitrogen budget
Critical load
Ammonia
Nitrogen oxides

## ABSTRACT

We present a national-scale model analysis on the sources and processes of inorganic nitrogen deposition over China using the GEOS-Chem model at 1/2° × 1/3° horizontal resolution. Model results for 2008–2012 are evaluated with an ensemble of surface measurements of wet deposition flux and gaseous ammonia ($NH_3$) concentration, and satellite measurements of tropospheric $NO_2$ columns. Annual total inorganic nitrogen deposition fluxes are simulated to be generally less than 10 kg N $ha^{-1}$ $a^{-1}$ in western China (less than 2 kg N $ha^{-1}$ $a^{-1}$ over Tibet), 15–50 kg N $ha^{-1}$ $a^{-1}$ in eastern China, and 16.4 kg N $ha^{-1}$ $a^{-1}$ averaged over China. Annual total deposition to China is 16.4 Tg N, with 10.2 Tg N (62%) from reduced nitrogen ($NH_x$) and 6.2 Tg N from oxidized nitrogen ($NO_y$). Domestic anthropogenic sources contribute 86% of the total deposition; foreign anthropogenic sources 7% and natural sources 7%. Annually 23% of domestically emitted $NH_3$ and 36% for $NO_x$ are exported outside the terrestrial land of China. We find that atmospheric nitrogen deposition is about half of the nitrogen input from fertilizer application (29.6 Tg N $a^{-1}$), and is much higher than that from natural biological fixation (7.3 Tg N $a^{-1}$) over China. A comparison of nitrogen deposition with critical load estimates for eutrophication indicates that about 15% of the land over China experiences critical load exceedances, demonstrating the necessity of nitrogen emission controls to avoid potential negative ecological effects.



## 1. Introduction

Human activities associated with energy and food production have greatly increased the availability of reactive nitrogen to the earth ecosystems, altering the natural nitrogen cycle (Galloway et al., 2004; Fowler et al., 2013). Excess nitrogen inputs can cause adverse ecological effects including soil acidification, plant biodiversity reduction, and eutrophication in the ecosystems (Bouwman et al., 2002; Bowman et al., 2008; Stevens et al., 2004). Atmospheric deposition represents an important source of reactive nitrogen to ecosystems (Galloway et al., 2004; Fowler et al., 2013). Rapid industrialization, urbanization, and agricultural development in China have made the country a hotspot of nitrogen deposition over

* Corresponding author.
*E-mail address:* zhanglg@pku.edu.cn (L. Zhang).

http://dx.doi.org/10.1016/j.atmosenv.2017.01.018
1352-2310/

the world, leading to increasing concerns on the threat to vulnerable ecosystems (Kim et al., 2011; Liu et al., 2011, 2013; Luo et al., 2014).

Nitrogen deposition mainly originates from emissions of nitrogen oxides ($NO_x \equiv NO + NO_2$) and ammonia ($NH_3$) with both anthropogenic and natural sources. $NO_x$ in the atmosphere can be oxidized to nitric acid ($HNO_3$), and $NH_3$ neutralizes sulfuric acid ($H_2SO_4$) and $HNO_3$ to form ammonium sulfate and ammonium nitrate aerosols. Their ultimate fates are return to the surface by wet and dry deposition processes. A number of studies have examined the magnitude and variability of nitrogen deposition over China (Lv and Tian, 2007, 2014; Pan et al., 2012; Jia et al., 2014; Xu et al., 2015; Zhu et al., 2015), nearly all based on measurements of nitrogen wet deposition fluxes and surface concentrations. Considerable uncertainties, however, exist when interpolating those measurements at limited monitoring sites to a national scale (Liu et al., 2015; He et al., 2015). In addition, dry deposition, often estimated by an inferential method with the deposition fluxes calculated as products of measured surface concentrations and model estimated dry deposition velocities, includes only part of nitrogen species that are regularly monitored (Clarke et al., 1997; Vet et al., 2014). A better understanding of the sources and processes of nitrogen deposition is needed to assess the current situation of nitrogen pollution and its potential ecological effects over China.

Chemical transport models (CTMs) with the capability of linking nitrogen sources with deposition provide a perspective complementary to measurements. Models have been applied to analyze nitrogen deposition over the globe (Dentener et al., 2006; Sanderson et al., 2008), the United States (Zhang et al., 2012a; Ellis et al., 2013), and Europe (Simpson et al., 2014). Such applications over China have been mainly focused on simulating acid deposition (Wang et al., 2008; Zhao et al., 2009; Ge et al., 2014). Here we use the GEOS-Chem CTM at horizontal resolution of $1/2^\circ \times 1/3^\circ$ over Asia to simulate nitrogen deposition to China for the years 2008–2012, and to better quantify contributions from dry versus wet deposition of each species and from domestic, foreign anthropogenic and natural sources. We also estimate the terrestrial nitrogen inputs via fertilizer application and biological fixation, and compare with estimates of nitrogen critical load (defined as a threshold of nitrogen input below which the ecosystem damage will not occur (Nilsson and Grennfelt, 1988)) in China to identify the potential exceeding areas.

## 2. Model description and method

### 2.1. Model description

We use the GEOS-Chem CTM (http://geos-chem.org) driven by GEOS-5 assimilated meteorological data from the Goddard Earth Observing System (GEOS) of the NASA Global Modeling and Assimilation Office (GMAO). The GEOS-5 data have a temporal resolution of 6 h (3 h for surface variables and mixing layer depth) and horizontal resolution of $1/2^\circ \times 1/3^\circ$. We use a nested version of GEOS-Chem with the native $1/2^\circ \times 1/3^\circ$ horizontal resolution over East Asia (70–150°E, 11° S–55°N) and $4^\circ \times 5^\circ$ for rest of the world (Chen et al., 2009). The nested GEOS-Chem model has been previously applied to investigate nitrogen deposition to the northwestern Pacific (Zhao et al., 2015) and to the United States (Zhang et al., 2012a; Ellis et al., 2013).

The model simulates a detailed tropospheric ozone-$NO_x$-hydrocarbon-aerosol chemistry (Bey et al., 2001; Park et al., 2004; Mao et al., 2010). Gas and aerosol-phase chemistry are coupled through heterogeneous aerosol chemistry parameterized as reactive uptake coefficients (Jacob, 2000), aerosol effects on photolysis rates (Martin et al., 2003), and gas-aerosol partitioning of total $NH_3$ and $HNO_3$ using the ISORROPIA II thermodynamic equilibrium model (Fountoukis and Nenes, 2007). The model parameterization of wet deposition, which includes both convective updraft and large-scale precipitation scavenging, is described by Liu et al. (2001) for aerosols, and by Mari et al. (2000) and Amos et al. (2012) for soluble gases. Dry deposition calculation follows a standard resistance-in-series model described in Wesely (1989) for gases and Zhang et al. (2001) for aerosols. The model here does not account for land-atmosphere bi-directional $NH_3$ exchange (Massad et al., 2010; Sutton et al., 2013), and the fluxes are parameterized as uncoupled emission and dry deposition processes.

Anthropogenic emissions over China are from the Multi-Resolution Emission Inventory of China (MEIC, http://meicmodel.org) except for $NH_3$ emissions, which are from the Regional Emission in Asia (REAS-v2) inventory for 2008 (Kurokawa et al., 2013) with an updated seasonality described in Zhao et al. (2015) (Fig. 1). Our previous work (Zhao et al., 2015) and Fig. 2 (shown below) indicate that model simulations with this $NH_3$ emission estimate are in good agreement with available surface measurements over China. Natural sources of reactive nitrogen in the model, including lightning, soil, and biomass burning, have been described in Zhao et al. (2015) in detail. We conduct model simulations for the years 2008–2012. The MEIC anthropogenic $NO_x$ emissions include inter-annual changes for 2008–2010, and the 2010 emissions are used for the simulation afterwards. Our results would thus underestimate the inter-annual variability of nitrogen deposition, as recent studies showed that Chinese $NO_x$ emissions might peak in 2011 and start declining in 2012 (Mijling et al., 2013; Liu et al., 2016). Here we focus on the averaged model results over the five years. Fig. 1 shows the spatial distributions of annual $NH_3$ and $NO_x$ emissions over China. Total $NH_3$ and $NO_x$ emissions over China are, respectively, 13.0 Tg N $a^{-1}$ (per annum) and 9.42 Tg N $a^{-1}$; 96% of $NH_3$ and 92% of $NO_x$ emissions are anthropogenic.

### 2.2. Nitrogen inputs from fertilizer application and natural biological fixation

To assess the relative contribution of different nitrogen sources over China, we compare atmospheric deposition with other terrestrial nitrogen inputs from fertilizer application and natural fixation. We use the dataset of chemical fertilizer application and manure production from Potter et al. (2010) at a native resolution of $0.5^\circ \times 0.5^\circ$, and we regrid it to the model resolution. The dataset provides spatially resolved annual total chemical fertilizer inputs by mapping national-level fertilizer use statistics from International Fertilizer Industry Association (IFA) for 2002 to various croplands of Monfreda et al. (2008), and annual manure production rates estimated based on the livestock density distribution of Wint and Robinson (2007). We scale the 2002 fertilizer use data to 2010 values for each province based on the China Rural Statistical Year Book following Gu et al. (2015), leading to a total input of 29.4 Tg N $a^{-1}$ as chemical fertilizer over China. We also follow Sheldrick et al. (2003) and Hudman et al. (2012) by assuming that 37% of manure nitrogen is applied to soils, resulting in a nitrogen input of 8.0 Tg N $a^{-1}$ as manure. To avoid double counting the nitrogen fluxes associated with fertilizer application, we subtract the fertilizer-induced $NH_3$ emissions (7.8 Tg N $a^{-1}$ from both chemical and manure fertilizers in the REAS-2 inventory) from the total fertilizer use of 37.4 Tg N $a^{-1}$ (29.4 plus 8.0 Tg N $a^{-1}$). The resulting net nitrogen inputs to China from fertilizer application are 29.6 Tg N $a^{-1}$.

We further calculate the biological nitrogen fixation rates as a function of annual net primary production (NPP) following the formula given in Koven et al. (2013), which is also used in the Community Land Model version 4 (CLM v4):

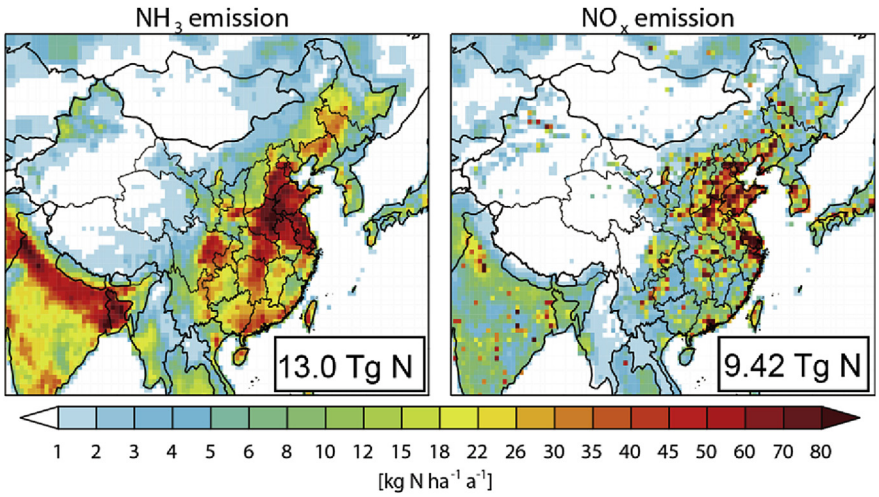


**Fig. 1.** Spatial distribution of $NH_3$ (left) and $NO_x$ (right) emissions averaged over 2008–2012. Annual emission totals in China are shown inset.

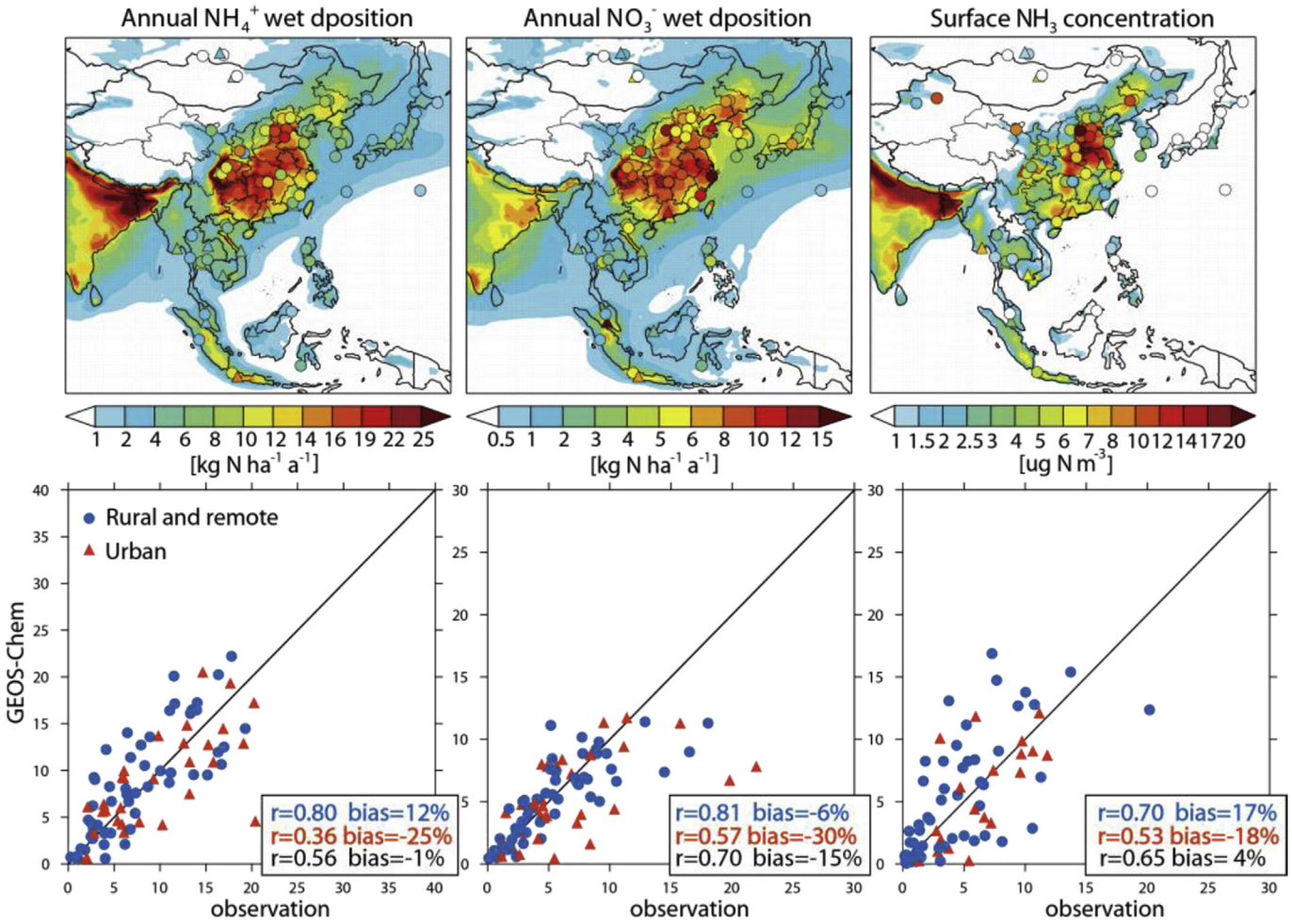


**Fig. 2.** Annual wet deposition fluxes of $NH_4^+$ (left) and $NO_3^-$ (middle), and mean surface $NH_3$ concentrations (right) averaged for 2008–2012. The GEOS-Chem model results are compared with an ensemble of measurements (as described in the text) overplotted (top panels) and as scatter-plots (bottom panels). In all panels, the urban sites are denoted as red triangles while the remote and rural sites are shown as blue circles. Correlation coefficients (r) and normalized mean biases for the urban sites (red), rural/remote sites (blue), and all sites (black) are shown inset. (For interpretation of the references to colour in this figure legend, the reader is referred to the web version of this article.)

$$NF_{fix} = 1.8 \times \left(1 - e^{-0.003 \times NPP}\right) \quad (1)$$

The annual NPP products from the MODIS satellite instrument are used and averaged over the years 2008–2012 (data available at http://neo.sci.gsfc.nasa.gov/). Using this formula, we estimate that the global biological nitrogen fixation is about 114.5 Tg N $a^{-1}$, in consistency with the range of 100–290 Tg N $a^{-1}$ reported by Cleveland et al. (1999). Biological nitrogen fixation over China is relatively small (7.34 Tg N $a^{-1}$; as will be shown in Fig. 5), since most of the fixation occurs in tropical ecosystems (Cleveland et al., 1999).

### 2.3. Critical load thresholds

The critical load is defined as a quantitative estimate of pollution exposure below which significant harmful effects do not occur according to present knowledge (Nilsson and Grennfelt, 1988). Mapping of nitrogen critical load for eutrophication used in China was based on the steady state mass balance (SSMB) method (Duan et al., 2001) and refined by Zhao et al. (2011). Zhao et al. (2011) reported nitrogen critical load estimates for both eutrophication and acidification, and here we focus on the effect of eutrophication. The nitrogen critical load for eutrophication ($CL_N$) is derived using the formula:

$$CL_N = N_i + N_u + N_{de} + Q \times \left[NO_3^-\right]_{crit} \quad (2)$$

where $N_i$ is the long-term averaged nitrogen immobilization rate in soil, $N_u$ is the net uptake rate by plants, $N_{de}$ is the denitrification rate in soil, Q is the water runoff flux leaving the root zone, and $[NO_3^-]_{crit}$ is the critical concentration of $[NO_3^-]$ in runoff above which harmful effects would occur for the ecosystem. Details of the land vegetation type, soil property, and critical concentration have been described in Duan et al. (2002, 2004). The nitrogen critical loads have been estimated for each terrestrial ecosystem over China. The critical load values are mapped to the resolution of 36 km × 36 km, and here we remap them to the model 1/2° × 1/3° resolution for comparison with the nitrogen deposition.

## 3. Results and discussion

### 3.1. Wet deposition fluxes and gas concentrations

We first evaluate the model simulation of nitrogen deposition over China using available surface measurements of wet deposition flux and ammonia gas concentration, as well as tropospheric $NO_2$ column measurements from the OMI satellite instrument. Due to a lack of direct dry deposition measurements, we rely on the measurements of nitrogen gas concentrations for the evaluation of dry deposition simulation. An ensemble of surface data is complied from the Acid Deposition Monitoring Network in East Asia (EANET; data available at http://www.eanet.asia/index.html) for 2008–2012, a nationwide measurement network over China for 2011–2012 (Xu et al., 2015), and 10 sites monitored by Chinese Academy of Sciences in North China for 2008–2010 (Pan et al., 2012). We select the measurement sites that have at least one-year continuous measurements. These include 87 (31 urban and 56 rural or remote) sites for wet deposition fluxes, and 79 (21 urban and 58 rural/remote) sites for $NH_3$ concentrations.

Fig. 2 compares the model simulated annual nitrogen wet deposition fluxes and $NH_3$ concentrations averaged over 2008–2012 with the ensemble of surface measurements. We calculate the correlation coefficient ($r$) and the normalized mean bias ($NMB = \sum_{i=1}^{N}(M_i - O_i)/\sum_{i=1}^{N} O_i$) between the observed (O) and modeled (M) values over the $N$ sites for the model evaluation. The model generally reproduces the measured spatial distributions of $NH_4^+$ wet deposition fluxes ($r = 0.56$) and surface $NH_3$ gas concentrations ($r = 0.65$), with only small annual biases (−1% for $NH_4^+$ wet deposition fluxes and 4% for $NH_3$ concentrations). The model also captures measured $NO_3^-$ wet deposition fluxes ($r = 0.70$) with a mean bias of −15%, mainly due to some underestimates of deposition fluxes measured at the urban sites. We do not have surface $NO_2$ concentration measurements available for the studying period. However, a comparison of model simulated vs. OMI observed tropospheric $NO_2$ columns, shows a good agreement over China ($r = 0.95$, bias = −6.8%; Supplementary Material Fig. S1). We shall also acknowledge that most of those wet deposition measurements are actually bulk deposition, which include both wet deposition and part of dry deposition (Xu et al., 2015).

The simulated nitrogen wet deposition is about 10.0 kg N $ha^{-1}$ $a^{-1}$ averaged over the terrestrial land of China, with 66% contributed by reduced nitrogen ($NH_4^+$). This is comparable to previous studies based on spatial interpolation of surface measurements that reported mean wet deposition flux to China in the range of 9.88–13.9 kg N $ha^{-1}$ $a^{-1}$ (Lv and Tian, 2007; Jia et al., 2014; Zhu et al., 2015), and 55%–78% contribution from $NH_4^+$ wet deposition (Lv and Tian, 2007; Pan et al., 2012; Zhu et al., 2015).

### 3.2. Deposition processes and source attribution

We examine the different sources and processes contributing to nitrogen deposition to China by using the GEOS-Chem model results over 2008–2012. Simulated interannual variability is relatively small on the national scale, with annual deposition fluxes ranging 15.5–17.5 Tg N $a^{-1}$ over China in the 5 years.

Fig. 3 shows the spatial distribution of annual wet and dry deposition fluxes of reduced ($NH_x$) and oxidized ($NO_y$) nitrogen, and Table 1 summarizes the annual total deposition amounts from individual species and from each process over China. For all deposition patterns, there is a sharp gradient from west to east, mainly driven by the emission patterns for both $NH_3$ and $NO_x$ (Fig. 1). On the national scale, more $NH_x$ is removed through wet deposition than dry deposition (6.6 versus 3.6 Tg N $a^{-1}$). The higher wet deposition than dry deposition fluxes for $NH_x$ are particularly distinct over southeastern China because of the high annual precipitation amounts over that region (Fig. S2). $NH_x$ dry deposition is preferentially through gaseous $NH_3$ (72% of $NH_x$ dry deposition; 2.6 Tg N $a^{-1}$) reflecting its higher deposition velocity than ammonium aerosol. For $NO_y$, wet and dry depositions are comparable (3.4 versus 2.8 Tg N $a^{-1}$). Annually $HNO_3$ accounts for 61% of the $NO_y$ dry deposition, $NO_2$ 11%, isoprene nitrates 4.6%, and $NO_3^-$ aerosol 18%.

We can see that dry deposition accounts for 35% of the $NH_x$ deposition, 45% of the $NO_y$ deposition, and 39% of the total inorganic nitrogen deposition to China. Xu et al. (2015) estimated that dry deposition accounted for 52% of the total inorganic nitrogen deposition by using measurements at the nationwide network which we have included in the model evaluation. If sampling at these site locations, our model results also suggest a dry deposition contribution of 45% to the total deposition. Pan et al. (2012) and Xu et al. (2015) have also shown that more $NH_x$ is deposited over China than $NO_y$. This is supported by our model results with deposition of $NH_x$ contributing 62% of the total nitrogen deposition, driven by the higher $NH_3$ emissions than $NO_x$ on the national scale.

Fig. 4 shows the simulated spatial distribution of annual total (wet and dry) nitrogen deposition over China. Nitrogen deposition is generally less than 10 kg N $ha^{-1}$ $a^{-1}$ in western China, and 15–50 kg N $ha^{-1}$ $a^{-1}$ in eastern China. The lowest values occur over Tibet with deposition fluxes less than 2 kg N $ha^{-1}$ $a^{-1}$. High

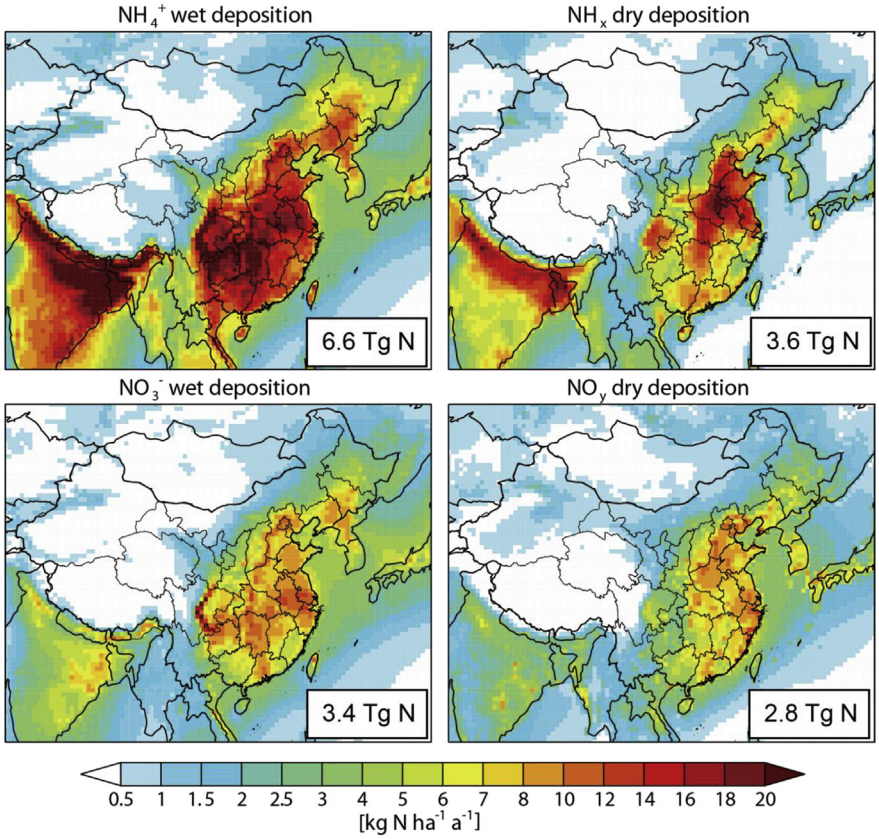


**Fig. 3.** Simulated annual total $NH_4^+$ wet deposition, $NH_x$ dry deposition, $NO_3^-$ wet deposition, and $NO_y$ dry deposition averaged over 2008–2012. Annual totals over China from each process are shown inset.

**Table 1**
Nitrogen deposition to China.[a]

| | Deposition process | Deposition (Tg N $a^{-1}$) |
|---|---|---|
| $NH_x$ | Total | 10.2 |
| | Wet $NH_4^+$ | 6.6 |
| | Dry $NH_3$ | 2.6 |
| | Dry $NH_4^+$ aerosol | 1.0 |
| $NO_y$ | Total | 6.2 |
| | Wet $NO_3^-$ | 3.4 |
| | Dry $HNO_3$ | 1.7 |
| | Dry $NO_2$ | 0.3 |
| | Dry isoprene nitrates[b] | 0.13 |
| | Dry $N_2O_5$ | 0.057 |
| | Dry PANs[c] | 0.058 |
| | Dry $NO_3^-$ aerosol | 0.5 |
| | Dry alkyl nitrates | 0.009 |

[a] Annual nitrogen deposition fluxes averaged over 2008–2012 simulated by the GEOS-Chem model.

[b] Isoprene nitrates are produced from the oxidation of biogenic isoprene and are removed by dry and wet deposition at the same rate as $HNO_3$ in the model following Zhang et al. (2012a).

[c] Peroxyacetyl nitrate (PAN) and higher peroxyacyl nitrates.

nitrogen deposition fluxes are simulated in central China (such as Henan, Shandong, Jiangsu, Anhui provinces) and the western ridge of Sichuan Basin, where regional mean deposition values can exceed 40 kg N $ha^{-1}$ $a^{-1}$. Previous simulations of nitrogen deposition at the global scale have shown that eastern China is one of the highest depositing regions with fluxes generally exceeding 20 kg N $ha^{-1}$ $a^{-1}$ in the 2000s (Dentener et al., 2006; Lamarque et al., 2013). Our results at a higher spatial resolution are consistent with those global model estimates, and also well capture the available measurements (Fig. 2).

We separate contributions to nitrogen deposition from the Chinese domestic anthropogenic, foreign anthropogenic, and natural sources. Two sensitivity simulations are conducted for the year 2012: (1) with all anthropogenic emissions in China shut off and (2) with global all anthropogenic emissions shut off. Contributions from different sources are then estimated by their differences with the standard simulation for 2012. As shown in Fig. 4, annual total $NH_x$ and $NO_y$ deposition fluxes to China are respectively 10.7 Tg N $a^{-1}$ and 6.76 Tg N $a^{-1}$ in 2012. 89% of $NH_x$ deposition (9.51 Tg N $a^{-1}$) and 82% of $NO_y$ deposition (5.57 Tg N $a^{-1}$) are attributed to domestic anthropogenic emissions. About 6–7% of $NH_x$ and $NO_y$ deposition are imported from outside contributed by foreign anthropogenic emissions. Natural sources account for the rest 4% of $NH_x$ deposition, 10% of $NO_y$ deposition, and 7% of the total deposition.

Compared with nitrogen emissions, we find in the model that 2.97 Tg N as $NH_x$ and 3.55 Tg N as $NO_y$ are exported outside the terrestrial land of China annually, which account for 24% and 36% of the $NH_3$ and $NO_x$ emissions, respectively. A large fraction of the exported $NH_x$ and $NO_y$ is deposited to the adjacent northwestern Pacific. Zhao et al. (2015) showed that over 90% of nitrogen deposition to the Chinese seas of the northwestern Pacific originated from nitrogen sources over land in China, and Sanderson et al. (2008) found a much smaller export fraction of 12% for $NO_y$ over East Asia covering China, Korea, Japan, and the adjacent ocean. We find similar export fractions (6% for $NH_3$ and 10% for $NO_x$) when considering the East Asian domain.

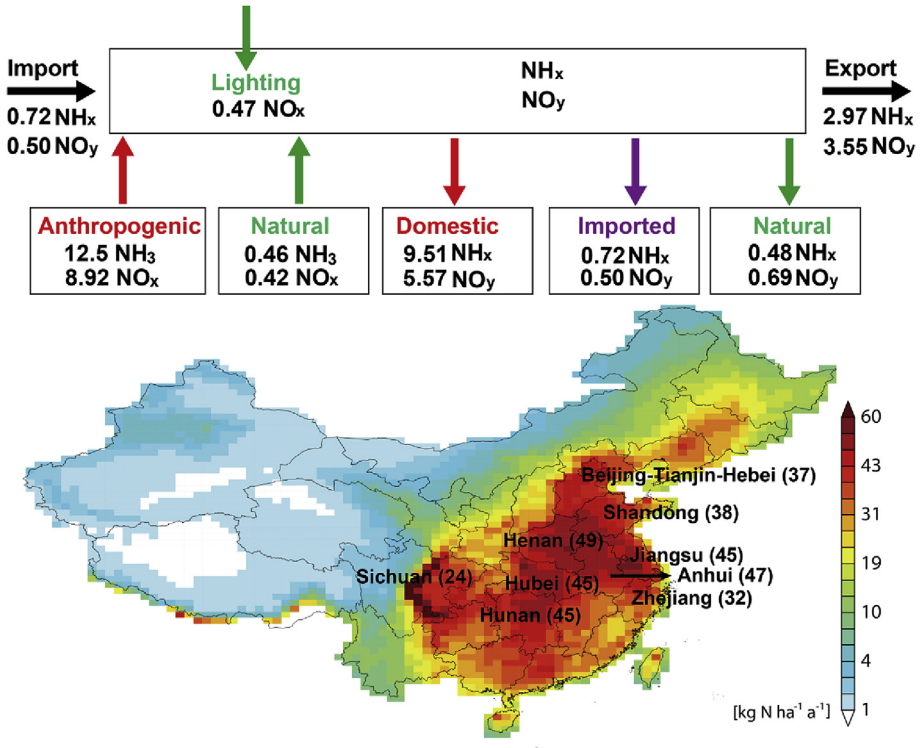


**Fig. 4.** Sources and sinks of inorganic nitrogen over China as simulated by the GEOS-Chem model for 2012. The map shows spatial distribution of annual total nitrogen deposition ($NH_x$ and $NO_y$, wet and dry), with the averaged deposition values in unit of kg N $ha^{-1}$ $a^{-1}$ over major deposition provinces listed. Also shown are the emission, deposition, imported, and exported nitrogen fluxes over China in unit of Tg N $a^{-1}$ as computed by model sensitivity simulations described in the text.

### 3.3. Nitrogen critical load exceedance

We compare in Fig. 5 annual atmospheric deposition (Fig. 5a) with other terrestrial nitrogen inputs from natural biological fixation (Fig. 5b) and fertilizer application (Fig. 5c) as described in Section 2.2. On the national scale nitrogen inputs from atmospheric deposition, natural biological fixation, and fertilizer application are, respectively, 16.4, 7.3, and 29.6 Tg N $a^{-1}$. For the spatial distribution, nitrogen inputs from fertilizer application are highly concentrated over the croplands in central China including the southern Hebei, Henan, and Shandong provinces, with nitrogen fluxes reach 300 kg N $ha^{-1}$ $a^{-1}$. Atmospheric deposition is much more widely distributed, and it is generally a factor of 2–5 higher than natural biological nitrogen fixation.

Fig. 5 also shows the critical load for eutrophication estimated by the SSMB method of Zhao et al. (2011) (Fig. 5d), and exceedances calculated as the differences between nitrogen deposition and critical loads at the model 1/2° × 1/3° resolution (Fig. 5e). We find that 15% of the country's terrestrial land is receiving nitrogen deposition greater than the critical load, mainly located in northeastern, central, and southern China. The critical load exceedances can reach more than 30 kg N $ha^{-1}$ $a^{-1}$ due to high deposition rates to sensitive ecosystems. Many of those areas are also experiencing exceedances of critical load for soil eutrophication as found by Zhao et al. (2011) using model simulated atmospheric deposition of nitrogen and sulfur.

While such comparisons demonstrate the relative importance of atmospheric deposition, some large uncertainties need to be considered. The critical load calculation is strongly influenced by parameters used in the SSMB method (Section 2.3), such as plant uptake rate, weathering rate, and denitrification rate, all subject to considerable uncertainties (Duan et al., 2001). It is also limited by the method itself as a sample mass balance model of reality (Posch et al., 2015). An empirical critical load map compiled by Liu et al. (2011) using field observations over various ecosystems shows a spatial distribution very similar to the SSMB estimates, but critical load values can differ by a factor of 2–3 for some ecosystems.

Uncertainties also exist in current Chinese $NH_3$ emission estimates with a large range of 7.9–13.2 Tg N $a^{-1}$ (e.g., Streets et al., 2003; Huang et al., 2012; Paulot et al., 2014) or possible underestimates of non-agricultural sources (Chang et al., 2016; Pan et al., 2016). The REAS-v2 anthropogenic $NH_3$ emissions (12.5 Tg N $a^{-1}$) that we used here are at the high end, mainly because of a higher estimate of $NH_3$ from fertilizer application (7.8 Tg N $a^{-1}$) than other studies (e.g., 3.2 Tg N $a^{-1}$ in Huang et al. (2012)). Although the model with this $NH_3$ emission inventory successfully reproduces available measurements of wet deposition fluxes and surface concentrations, there is a lack of direct in situ measurements (e.g., eddy-covariance flux measurements) to evaluate model simulated dry deposition fluxes. In addition, by not considering the land-atmosphere bi-directional $NH_3$ exchange and instead subtracting fertilizer-induced $NH_3$ emissions from its use amount, our results likely provide an upper bound estimate of atmospheric inorganic nitrogen deposition, however, wet deposition of dissolved organic nitrogen, which is estimated to be about 28% of the nitrogen wet deposition in China (Zhang et al., 2012b), is not included here as well. Future studies are thus needed to reduce these uncertainties for better supporting environmental policy and decision-making.

## 4. Conclusions

In summary, we have presented a national-scale model analysis of the sources and processes contributing to inorganic nitrogen deposition over China. We simulate the annual nitrogen deposition fluxes to China averaged over 2008–2012 using the GEOS-Chem

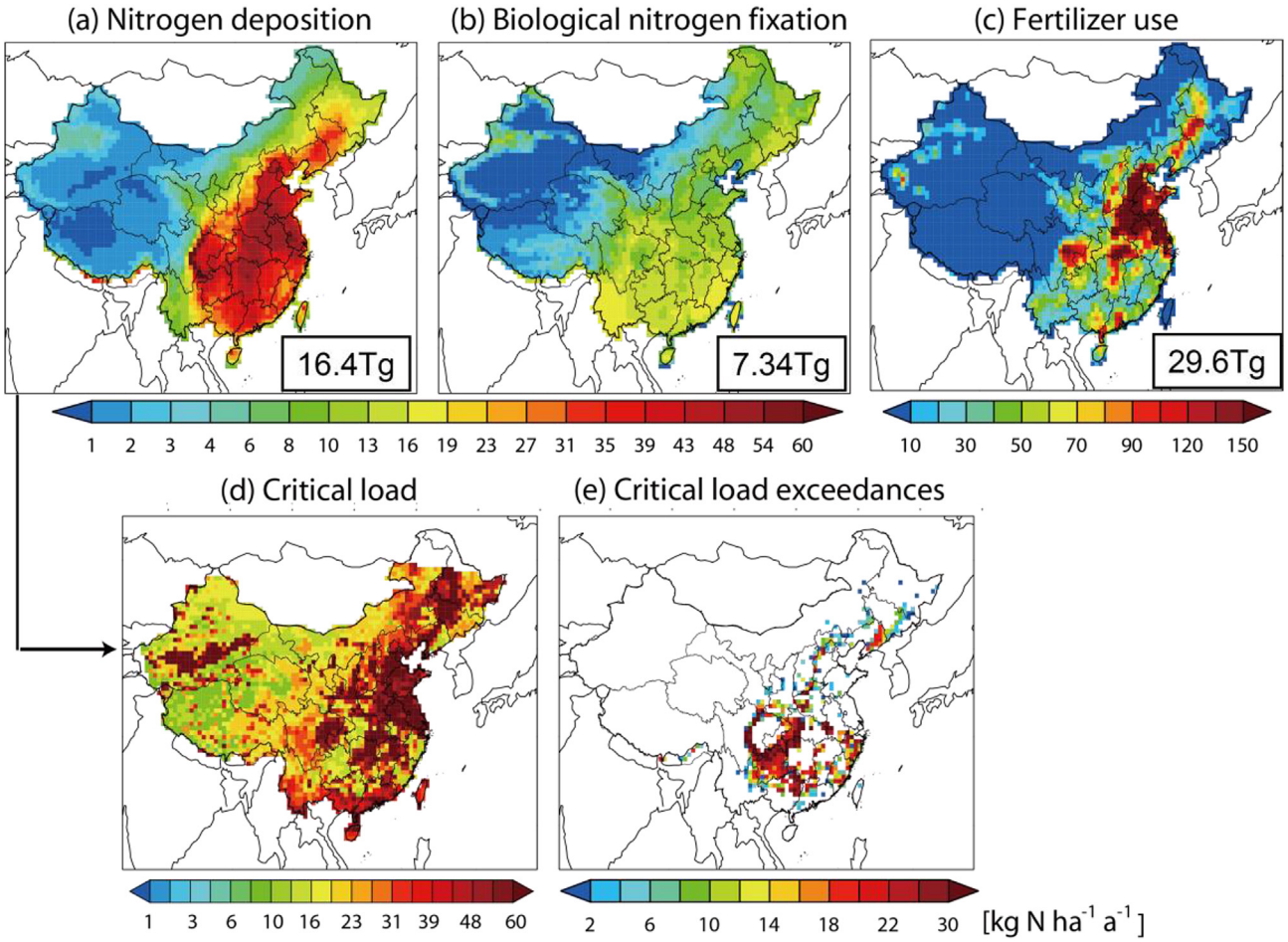


**Fig. 5.** Terrestrial nitrogen input and critical load exceedance over China. Nitrogen inputs including: (a) nitrogen deposition, (b) biological nitrogen fixation, and (c) fertilizer use. Values inset are corresponding annual totals over China. (d) Estimates of nitrogen critical load for eutrophication. (e) Critical load exceedance calculated as nitrogen deposition minus critical load. Areas with no exceedance in China are shown in white.

model at 1/2° × 1/3° horizontal resolution. Model results are evaluated with an ensemble of surface measurements of nitrogen wet deposition flux and ammonia concentration, as well as satellite observed tropospheric $NO_2$ columns; all show reasonable agreements.

The model provides a comprehensive view on the sources and sinks of inorganic nitrogen at fine spatial resolution. We show that annual nitrogen deposition fluxes are generally less than 10 kg N $ha^{-1}$ $a^{-1}$ in western China, 15–50 kg N $ha^{-1}$ $a^{-1}$ in eastern China, and about 16.4 kg N $ha^{-1}$ $a^{-1}$ averaged over China. On the national scale 62% of the total nitrogen deposition to China (10.2 Tg N) is contributed by reduced nitrogen ($NH_x$), and 39% of the total deposition is through dry deposition. We find that domestic anthropogenic sources have dominant contributions to nitrogen deposition over China (89% of $NH_x$ deposition, 82% of $NO_y$ deposition, and 86% of the total deposition). Foreign anthropogenic emissions contribute about 7% of $NH_x$ and $NO_y$ deposition. Natural sources (e.g., lightning, soil, and biomass burning) account for the rest 4% of $NH_x$ deposition and 10% of $NO_y$ deposition. Annually 2.97 Tg N as $NH_x$ and 3.55 Tg N as $NO_y$ are exported that are 22% and 36% of the domestic $NH_3$ and $NO_x$ emissions.

We also find that the annual total nitrogen deposition to China (16.4 Tg N $a^{-1}$, deposition flux integrated over the grid cells covering the land of China ~$10^7$ $km^2$) is about half of the nitrogen input from fertilizer application (29.6 Tg N $a^{-1}$), and much higher than natural biological fixation (7.3 Tg N $a^{-1}$). Comparing with estimates of nitrogen critical load for eutrophication, we show that about 15% of the land over China is now receiving nitrogen deposition higher than the critical loads. While we acknowledge that such a comparison has large uncertainties in both estimates of nitrogen deposition and critical load, it provides a scientific basis for understanding the condition of nitrogen nutrient imbalance and pointing out regions where emission control measures to reduce nitrogen deposition are important to avoid negative effects from critical load exceedances.

## Acknowledgments

This work was funded by China's National Basic Research Program (2014CB441303), and by the National Natural Science Foundation of China (41205103, 41475112, 41425007, and 41405144).

## Appendix A. Supplementary data

Supplementary data related to this article can be found at http://dx.doi.org/10.1016/j.atmosenv.2017.01.018.

## References

Amos, H.M., Jacob, D.J., Holmes, C.D., Fisher, J.A., Wang, Q., Yantosca, R.M., Corbitt, E.S., Galarneau, E., Gustin, M.S., Steffen, A., Schauer, J.J., Graydon, J.A., St Louis, V.L., Talbot, R.W., Edgerton, E.S., Zhang, Y., Sunderland, E.M., 2012. Gas-particle partitioning of atmospheric Hg(II) and its effect on global mercury

deposition. Atmos. Chem. Phys. 12, 591–603.
Bey, I., Jacob, D.J., Yantosca, R.M., Logan, J.A., Field, B.D., Fiore, A.M., Li, Q.B., Liu, H.G.Y., Mickley, L.J., Schultz, M.G., 2001. Global modeling of tropospheric chemistry with assimilated meteorology: model description and evaluation. J. Geophys Res.-Atmos. 106, 23073–23095.
Bouwman, A.F., Van Vuuren, D.P., Derwent, R.G., Posch, M., 2002. A global analysis of acidification and eutrophication of terrestrial ecosystems. Water Air Soil Poll. 141, 349–382.
Bowman, W.D., Cleveland, C.C., Halada, L., Hresko, J., Baron, J.S., 2008. Negative impact of nitrogen deposition on soil buffering capacity. Nat. Geosci. 1, 767–770.
Chang, Y., Liu, X., Deng, C., Dore, A.J., Zhuang, G., 2016. Source apportionment of atmospheric ammonia before, during, and after the 2014 APEC summit in Beijing using stable nitrogen isotope signatures. Atmos. Chem. Phys. 16, 11635–11647.
Chen, D., Wang, Y., McElroy, M.B., He, K., Yantosca, R.M., Sager, P.L., 2009. Regional CO pollution and export in China simulated by the high-resolution nested-grid GEOS-chem model. Atmos. Chem. Phys. 9, 3825–3839.
Clarke, J., Edgerton, E., Martin, B., 1997. Dry deposition calculations for the clean air status and trends network. Atmos. Environ. 31, 3667–3678.
Cleveland, C.C., Townsend, A.R., Schimel, D.S., Fisher, H., Howarth, R.W., Hedin, L.O., Perakis, S.S., Latty, E.F., Von Fischer, J.C., Elseroad, A., Wasson, M.F., 1999. Global patterns of terrestrial biological nitrogen (N-2) fixation in natural ecosystems. Glob. Biogeochem. Cycles 13, 623–645.
Dentener, F., Drevet, J., Lamarque, J., Bey, I., Eickhout, B., Fiore, A.M., Hauglustaine, D., Horowitz, L., Krol, M., Kulshrestha, U., 2006. Nitrogen and sulfur deposition on regional and global scales: a multimodel evaluation. Glob. Biogeochem. Cycles 20 (4).
Duan, L., Xie, S., Zhou, Z., Ye, X., Hao, J., 2001. Calculation and Mapping of Critical Loads for S, N and Acidity in China, Acid Rain 2000. Springer, pp. 1199–1204.
Duan, L., Hao, J., Xie, S., Zhou, Z., Ye, X., 2002. Determining weathering rates of soils in China. Geoderma 110, 205–225.
Duan, L., Huang, Y., Hao, J., Xie, S., Hou, M., 2004. Vegetation uptake of nitrogen and base cations in China and its role in soil acidification. Sci. Total Environ. 330, 187–198.
Ellis, R., Jacob, D.J., Sulprizio, M.P., Zhang, L., Holmes, C., Schichtel, B., Blett, T., Porter, E., Pardo, L., Lynch, J., 2013. Present and future nitrogen deposition to national parks in the United States: critical load exceedances. Atmos. Chem. Phys. 13, 9083–9095.
Fountoukis, C., Nenes, A., 2007. ISORROPIA II: a computationally efficient thermodynamic equilibrium model for $K^+$-$Ca^{2+}$-$Mg^{2+}$-$NH_4^+$-$Na^+$-$SO_4^{2-}$-$NO_3^-$-$Cl^-$-$H_2O$ aerosols. Atmos. Chem. Phys. 7, 4639–4659.
Fowler, D., Coyle, M., Skiba, U., Sutton, M.A., Cape, J.N., Reis, S., Sheppard, L.J., Jenkins, A., Grizzetti, B., Galloway, J.N., 2013. The global nitrogen cycle in the twenty-first century. Phil. Trans. R. Soc. B 368 (1621), 20130164.
Galloway, J.N., Dentener, F.J., Capone, D.G., Boyer, E.W., Howarth, R.W., Seitzinger, S.P., Asner, G.P., Cleveland, C.C., Green, P.A., Holland, E.A., Karl, D.M., Michaels, A.F., Porter, J.H., Townsend, A.R., Vorosmarty, C.J., 2004. Nitrogen cycles: past, present, and future. Biogeochemistry 70, 153–226.
Ge, B., Wang, Z., Xu, X., Wu, J., Yu, X., Li, J., 2014. Wet deposition of acidifying substances in different regions of China and the rest of East Asia: modeling with updated NAQPMS. Environ. Pollut. 187, 10–21.
Gu, B., Ju, X., Chang, J., Ge, Y., Vitousek, P.M., 2015. Integrated reactive nitrogen budgets and future trends in China. Proc. Natl. Acad. Sci. 112, 8792–8797.
He, N., Zhu, J., Wang, Q., 2015. Uncertainty and perspectives in studies of atmospheric nitrogen deposition in China: a response to Liu et al. (2015). Sci. Total Environ. 520, 302–304.
Huang, X., Song, Y., Li, M., Li, J., Huo, Q., Cai, X., Zhu, T., Hu, M., Zhang, H., 2012. A high-resolution ammonia emission inventory in China. Glob. Biogeochem. Cycles 26.
Hudman, R., Moore, N., Mebust, A., Martin, R., Russell, A., Valin, L., Cohen, R., 2012. Steps towards a mechanistic model of global soil nitric oxide emissions: implementation and space based-constraints. Atmos. Chem. Phys. 12, 7779–7795.
Jacob, D.J., 2000. Heterogeneous chemistry and tropospheric ozone. Atmos. Environ. 34, 2131–2159.
Jia, Y., Yu, G., He, N., Zhan, X., Fang, H., Sheng, W., Zuo, Y., Zhang, D., Wang, Q., 2014. Spatial and decadal variations in inorganic nitrogen wet deposition in China induced by human activity. Sci. Rep. 4, 3763.
Kim, T.W., Lee, K., Najjar, R.G., Jeong, H.D., Jeong, H.J., 2011. Increasing N abundance in the northwestern pacific ocean due to atmospheric nitrogen deposition. Science 334, 505–509.
Koven, C., Riley, W., Subin, Z., Tang, J., Torn, M., Collins, W., Bonan, G., Lawrence, D., Swenson, S., 2013. The effect of vertically resolved soil biogeochemistry and alternate soil C and N models on C dynamics of CLM4. Biogeosciences 10, 7109–7131.
Kurokawa, J., Ohara, T., Morikawa, T., Hanayama, S., Janssens-Maenhout, G., Fukui, T., Kawashima, K., Akimoto, H., 2013. Emissions of air pollutants and greenhouse gases over Asian regions during 2000-2008: regional emission inventory in Asia (REAS) version 2. Atmos. Chem. Phys. 13, 11019–11058.
Lamarque, J.F., Dentener, F., Mcconnell, J., Ro, C.U., 2013. Multi-model mean nitrogen and sulfur deposition from the atmospheric chemistry and climate model intercomparison project (ACCMIP): evaluation historical and projected changes. Atmos. Chem. Phys. 13, 6247–6294.
Liu, F., Zhang, Q., Zheng, B., Tong, D., Yan, L., Zheng, Y., He, K., 2016. Recent reduction in NOx emissions over China: synthesis of satellite observations and emission inventories. Environ. Res. Lett. 11, 114002.
Liu, H.Y., Jacob, D.J., Bey, I., Yantosca, R.M., 2001. Constraints from Pb-210 and Be-7 on wet deposition and transport in a global three-dimensional chemical tracer model driven by assimilated meteorological fields. J. Geophys Res.-Atmos. 106, 12109–12128.
Liu, X.J., Duan, L., Mo, J., Du, E., Shen, J., Lu, X., Zhang, Y., Zhou, X., He, C., Zhang, F., 2011. Nitrogen deposition and its ecological impact in China: an overview. Environ. Pollut. 159, 2251–2264.
Liu, X.J., Xu, W., Pan, Y., Du, E., 2015. Liu et al. suspect that Zhu, et al. (2015) may have underestimated dissolved organic nitrogen (N) but overestimated total particulate N in wet deposition in China. Sci. Total Environ. 520, 300–301.
Liu, X.J., Zhang, Y., Han, W.X., Tang, A.H., Shen, J.L., Cui, Z.L., Vitousek, P., Erisman, J.W., Goulding, K., Christie, P., Fangmeier, A., Zhang, F.S., 2013. Enhanced nitrogen deposition over China. Nature 494, 459–462.
Luo, X., Tang, A., Shi, K., Wu, L., Li, W., Shi, W., Shi, X., Erisman, J., Zhang, F., Liu, X., 2014. Chinese coastal seas are facing heavy atmospheric nitrogen deposition. Environ. Res. Lett. 9, 095007.
Lv, C., Tian, H., 2007. Spatial and temporal patterns of nitrogen deposition in China: synthesis of observational data. J. Geophys. Res. Atmos. 112.
Lv, C., Tian, H., 2014. Half-century nitrogen deposition increase across China: a gridded time-series data set for regional environmental assessments. Atmos. Environ. 97, 68–74.
Mao, J., Jacob, D.J., Evans, M.J., Olson, J.R., Ren, X., Brune, W.H., St Clair, J.M., Crounse, J.D., Spencer, K.M., Beaver, M.R., Wennberg, P.O., Cubison, M.J., Jimenez, J.L., Fried, A., Weibring, P., Walega, J.G., Hall, S.R., Weinheimer, A.J., Cohen, R.C., Chen, G., Crawford, J.H., McNaughton, C., Clarke, A.D., Jaegle, L., Fisher, J.A., Yantosca, R.M., Le Sager, P., Carouge, C., 2010. Chemistry of hydrogen oxide radicals (HOx) in the Arctic troposphere in spring. Atmos. Chem. Phys. 10, 5823–5838.
Mari, C., Jacob, D.J., Bechtold, P., 2000. Transport and scavenging of soluble gases in a deep convective cloud. J. Geophys Res-Atmos 105, 22255–22267.
Martin, R.V., Jacob, D.J., Yantosca, R.M., Chin, M., Ginoux, P., 2003. Global and regional decreases in tropospheric oxidants from photochemical effects of aerosols. J. Geophys. Res. Atmos. 108.
Massad, R.-S., Nemitz, E., Sutton, M., 2010. Review and parameterisation of bi-directional ammonia exchange between vegetation and the atmosphere. Atmos. Chem. Phys. 10, 10359–10386.
Mijling, B., Van der A, R.J., Zhang, Q., 2013. Regional nitrogen oxides emission trends in East Asia observed from space. Atmos. Chem. Phys. 13, 12003–12012.
Monfreda, C., Ramankutty, N., Foley, J.A., 2008. Farming the planet: 2. Geographic distribution of crop areas, yields, physiological types, and net primary production in the year 2000. Glob. Biogeochem. Cycles 22 (1).
Nilsson, J., Grennfelt, P., 1988. Critical Loads for Sulphur and Nitrogen–Report from a Workshop Held at Skokloster, Sweden, 19-24 March, 1988. UN/ECE and Nordic Council of Ministers, p. 418.
Pan, Y., Tian, S., Liu, D., Fang, Y., Zhu, X., Zhang, Q., Zheng, B., Michalski, G., Wang, Y., 2016. Fossil fuel combustion-related emissions dominate atmospheric ammonia sources during severe haze episodes: evidence from 15N-stable isotope in size-resolved aerosol ammonium. Environ. Sci. Technol. 50, 8049–8056.
Pan, Y.P., Wang, Y.S., Tang, G.Q., Wu, D., 2012. Wet and dry deposition of atmospheric nitrogen at ten sites in northern China. Atmos. Chem. Phys. 12, 6515–6535.
Park, R.J., Jacob, D.J., Field, B.D., Yantosca, R.M., Chin, M., 2004. Natural and transboundary pollution influences on sulfate-nitrate-ammonium aerosols in the United States: implications for policy. J. Geophys Res-Atmos 109, D15204.
Paulot, F., Jacob, D.J., Pinder, R., Bash, J., Travis, K., Henze, D., 2014. Ammonia emissions in the United States, European Union, and China derived by high-resolution inversion of ammonium wet deposition data: interpretation with a new agricultural emissions inventory (MASAGE_NH3). J. Geophys. Res. Atmos. 119, 4343–4364.
Posch, M., Duan, L., Reinds, G.J., Zhao, Y., 2015. Critical loads of nitrogen and sulphur to avert acidification and eutrophication in Europe and China. Landsc. Ecol. 30, 487–499.
Potter, P., Ramankutty, N., Bennett, E.M., Donner, S.D., 2010. Characterizing the spatial patterns of global fertilizer application and manure production. Earth Interact. 14, 1–22.
Sanderson, M.G., Dentener, F.J., Fiore, A.M., Cuvelier, C., Keating, T.J., Zuber, A., Atherton, C.S., Bergmann, D.J., Diehl, T., Doherty, R.M., Duncan, B.N., Hess, P., Horowitz, L.W., Jacob, D.J., Jonson, J.E., Kaminski, J.W., Lupu, A., MacKenzie, I.A., Mancini, E., Marmer, E., Park, R., Pitari, G., Prather, M.J., Pringle, K.J., Schroeder, S., Schultz, M.G., Shindell, D.T., Szopa, S., Wild, O., Wind, P., 2008. A multi-model study of the hemispheric transport and deposition of oxidised nitrogen. Geophys Res. Lett. 35 (17).
Sheldrick, W., Syers, J.K., Lingard, J., 2003. Contribution of livestock excreta to nutrient balances. Nutr. Cycl. Agroecosyst. 66, 119–131.
Simpson, D., Andersson, C., Christensen, J.H., Engardt, M., Geels, C., Nyiri, A., Posch, M., Soares, J., Sofiev, M., Wind, P., 2014. Impacts of climate and emission changes on nitrogen deposition in Europe: a multi-model study. Atmos. Chem. Phys. 14, 6995–7017.
Stevens, C.J., Dise, N.B., Mountford, J.O., Gowing, D.J., 2004. Impact of nitrogen deposition on the species richness of grasslands. Science 303, 1876–1879.
Streets, D.G., Bond, T., Carmichael, G., Fernandes, S., Fu, Q., He, D., Klimont, Z., Nelson, S., Tsai, N., Wang, M.Q., 2003. An inventory of gaseous and primary

aerosol emissions in Asia in the year 2000. J. Geophys. Res. Atmos. 108.
Sutton, M.A., Reis, S., Riddick, S.N., Dragosits, U., Nemitz, E., Theobald, M.R., Tang, Y.S., Braban, C.F., Vieno, M., Dore, A.J., 2013. Towards a climate-dependent paradigm of ammonia emission and deposition. Philos. Trans. R. Soc. Lond. B Biol. Sci. 368, 20130166.
Vet, R., Artz, R.S., Carou, S., Shaw, M., Ro, C.-U., Aas, W., Baker, A., Bowersox, V.C., Dentener, F., Galy-Lacaux, C., 2014. A global assessment of precipitation chemistry and deposition of sulfur, nitrogen, sea salt, base cations, organic acids, acidity and pH, and phosphorus. Atmos. Environ. 93, 3–100.
Wang, Z., Xie, F., Sakurai, T., Ueda, H., Han, Z., Carmichael, G., Streets, D., Engardt, M., Holloway, T., Hayami, H., 2008. MICS-Asia II: model inter-comparison and evaluation of acid deposition. Atmos. Environ. 42, 3528–3542.
Wesely, M.L., 1989. Parameterization of surface resistances to gaseous dry deposition in regional-scale numerical-models. Atmos. Environ. 23, 1293–1304.
Wint, W., Robinson, T., 2007. Gridded Livestock of the World 2007. FAO, Roma (Italia).
Xu, W., Luo, X., Pan, Y., Zhang, L., Tang, A., Shen, J., Zhang, Y., Li, K., Wu, Q., Yang, D., Zhang, Y., Xue, J., Li, W., Li, Q., Tang, L., Lu, S., Liang, T., Tong, Y., Liu, P., Zhang, Q., Xiong, Z., Shi, X., Wu, L., Shi, W., Tian, K., Zhong, X., Shi, K., Tang, Q., Zhang, L., Huang, J., He, C., Kuang, F., Zhu, B., Liu, H., Jin, X., Xin, Y., Shi, X., Du, E., Dore, A., Tang, S., Collett Jr., J.L., Goulding, K., Sun, Y., Ren, J., Zhang, F., Liu, X., 2015. Quantifying atmospheric nitrogen deposition through a nationwide monitoring network across China. Atmos. Chem. Phys. 15, 12345–12360.
Zhang, L., Gong, S., Padro, J., Barrie, L., 2001. A size-segregated particle dry deposition scheme for an atmospheric aerosol module. Atmos. Environ. 35, 549–560.
Zhang, L., Jacob, D.J., Knipping, E.M., Kumar, N., Munger, J.W., Carouge, C.C., van Donkelaar, A., Wang, Y.X., Chen, D., 2012a. Nitrogen deposition to the United States: distribution, sources, and processes. Atmos. Chem. Phys. 12, 4539–4554.
Zhang, Y., Song, L., Liu, X., Li, W., Lü, S., Zheng, L., Bai, Z., Cai, G., Zhang, F., 2012b. Atmospheric organic nitrogen deposition in China. Atmos. Environ. 46, 195–204.
Zhao, Y., Duan, L., Lei, Y., Xing, J., Nielsen, C.P., Hao, J., 2011. Will PM control undermine China's efforts to reduce soil acidification? Environ. Pollut. 159, 2726–2732.
Zhao, Y., Duan, L., Xing, J., Larssen, T., Nielsen, C.P., Hao, J., 2009. Soil acidification in China: is controlling SO2 emissions enough? Environ. Sci. Technol. 43, 8021–8026.
Zhao, Y., Zhang, L., Pan, Y., Wang, Y., Paulot, F., Henze, D.K., 2015. Atmospheric nitrogen deposition to the northwestern Pacific: seasonal variation and source attribution. Atmos. Chem. Phys. 15, 10905–10924.
Zhu, J., He, N., Wang, Q., Yuan, G., Wen, D., Yu, G., Jia, Y., 2015. The composition, spatial patterns, and influencing factors of atmospheric wet nitrogen deposition in Chinese terrestrial ecosystems. Sci. Total Environ. 511, 777–785.